3D Modeling of Integrated Magnetics in High Frequency LLC Resonant Converters

Wayne. Water, and Junwei. Lu
Griffith University, School of Engineering
Nathan Campus, Brisbane, Australia
wayne.water@griffithuni.edu.au

***Abstract*— A novel structure of a planar transformer with magnetic integration is presented in this paper. The introduced transformer has a number of advantages and suitable for uses in the LLC resonant converter. The adjustment for the required resonant inductance of the LLC circuit is quite straightforward by controlling the distance of the magnetic bar to the magnetic core. However, it requires 3D FEM simulation of magnetic field analysis, in conjunction with the use of the energy method (due to the orthogonal structure of the windings and the insertion bar). Simulation results of the designed magnetics are presented in this paper. They are highly accurate according to the measurement results of a prototype. To optimize the resonant impedance, different insertion configurations of the magnetic bar have been investigated.**

***Index Terms*—LLC resonant converter, DC-DC power converter, finite element methods, magnetic integration, planar transformer.**

I. INTRODUCTION

There are four main components in the LLC resonant converter (shown in Figure.1): inductor (resonant inductor and magnetizing inductor), resonant capacitor, switches and transformer. The research work presented in this paper focuses on the magnetic components integration, which is specifically for inductors and transformers. Through magnetic integration, the total number of components is reduced and the converter system benefits from a reduction of both the overall volume and in manufacturing costs.

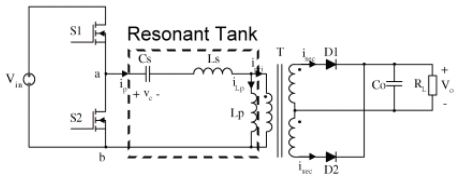

Figure 1. Half bridge LLC resonant circuit

A novel structure of an EE core planar transformer is presented in this paper. It has the advantages of being in low-profile, compact, and easily manufactured. Many researchers have studied magnetic integration [1]-[6]. In [3] and in their previous research works, several interesting designs has introduced. These mostly have the top-up structure of the magnetic integrated system by using an extra I shape magnetic material placed between two E-cores. Reference [4] has a similar top-up structure with the implementation of the EER cores. [5] uses two C cores, with one core behaving as the resonant inductor and the other core working as the transformer. Furthermore, [6] has a magnetic insertion inside the window of the transformer core. The presented design has advantages over the above designs for three main reasons. Firstly, it utilizes the existing space of the transformer in which to place the magnetic insertion bar. Secondly, there is fewer conduction losses due to the elimination of wires required for the resonant inductor; and finally, the resonant inductance is more controllable compared to the configuration which the magnetic insertion bar in the transformer window area.

II. DESIGN METHODOLOGY

A. Transformer Structure

The introduced planar transformer has dimensions of 53 mm x 38 mm x 17 mm and 36 mm x 8 mm x 2 mm for the magnetic bar. The magnetic bar is placed between the primary and secondary windings (with a distance of 1mm to the magnetic core), where primary is composed of Litz wires and secondary is copper plates. The first prototype was built with a power rating of 1 kW, output voltage of 36 V, nominal input voltage of 216 V (voltage ratio of 18:3), resonant frequency at 90 kHz, and an inductance ratio of 5, with the magnetizing inductance at 175 uH and the resonant inductance at 33 uH respectively.

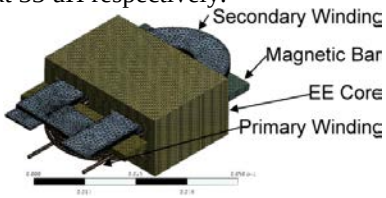

Figure 2. Introduced LLC transformer

B. Numerical Computation and Energy Method

A Finite Element Method (FEM) frequency domain based numerical technique was used to analyse the eddy current and magnetic flux distribution of the HF transformer. The nonlinear magnetic field of HF transformer can be determined by the following vector potential equation, where A and J are magnetic vector potential and current density respectively, ν is the magnetic reluctivity, and σ is the conductivity.The energy function is generalised from linear techniques.

$$\nabla \times (\nu \nabla \times A) + \sigma(\partial A / \partial t) = J. \quad (1)$$

The flux method can be used for magnetic field analysis of a simple structure [7]. The flux method uses Maxwell's

equations, which have a higher level of accuracy and predict magnetic behaviour in a frequency domain (in consideration of HF current effect). However, once the magnetic structure is more complicated, the energy method is a better solution and still provides acceptable results [8], [9]. Energy stored in the area is expressed as in (2), which governs the static domain, where μ is the permeability, H is the flux intensity and I_p is the current in the primary winding.

$$E_{Stored} = \frac{\mu}{2}\iiint H^2\, dv = \frac{1}{2}LI_p^2 \qquad (2)$$

III. Simulations and Testing Results

The first prototype was built with 1 mm distance between the magnetic bar and core, in which the relative permeability for both magnetics is 120. The measurements were obtained by using an HP 4285A (75 kHz to 30 MHz) precision LCR meter, where L_m is the magnetizing inductance and L_{eq} is the resonant inductance (also known as leakage inductance). A comparison result shown in Table I indicates that both simulation and measurement results are consistent with the design requirements.

TABLE I
The Inductance Validation of Simulations and Testing Results

	L_m (uH)	L_{eq} (uH)
Design requirement	175	33
3D simulation result	175.83	33.04
Testing result at 90 kHz – 25 ° C	173.34	32.16

Flux density simulation results under short circuit conditions and open circuit conditions are shown in Figure 3. The results show that the transformer is working under its saturation region in either a no-load or heavy-load situation (B_{sat}=450 mT at 25 ° C). In addition, the visualization of flux directions becomes easier with 3D simulation (the 2D simulation cannot achieve this in our novel structure). The flux direction illustration is shown in Figure 4, in which the flux circulates in an orthogonal angle from the core to the magnetic bar.

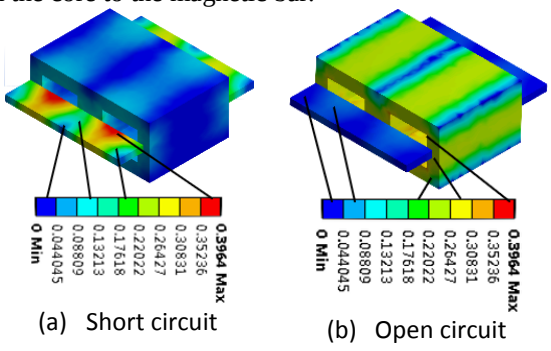

Figure 3. The 3D simulation of flux distribution

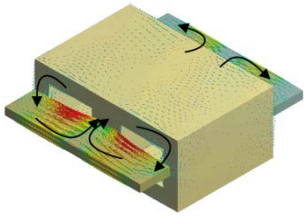

Figure 4.Illustration of flux direction

Furthermore, Table II shows the inductance comparison between different configurations by placing the magnetic bar in the window area between windings (the insertion goes through the window, which has a 90 degree angle compared to the introduced design). With the use of the magnetic bar in the same dimension, the maximum L_{eq} the system can achieve is 29.93 uH. By further increasing the length of magnetic insertion from 36 mm to 50.4 mm, the gain of L_{eq} is only 5.03 uH. In comparison, the maximum L_{eq} of the introduced design is 108.736 uH without the increase of the insertion length by the elimination of the air-gap (between core and insertion). Moreover, the simulation result of the eddy current (will be presented in the full paper) shows that with the magnetic insertion inside the window of the core, it causes a more severe proximity effect if primary windings have multiple stacks. The peak current density is double that of the case without the magnetic insertion. On the other hand, the presented design has little effect on the current distribution. The only drawback of the design is that it requires repeated simulation work and design processes before the prototype can be manufactured. This is because the L_m varied with every adjustment of air-gap distance. However, with recent advance in computation power, this will not be an issue.

TABLE II
The Inductance Comparison between Different Configurations of Magnetic Insertion Bar Arrangement

	Lm (uH)	Leq (uH)
No insertion	175.67	12.99
Insertion inside of core	175.81	29.93
Insertion outside of core	175.90	19.93
Insertion length increased to 50.4 mm	175.84	34.96

IV. References

[1] C. Deng, D. Xu, Y. Zhang, Y. Chen, Y. Okuma and K. Mino, "Impact of dielectric material on passive integration in LLC resonant converter," *Power Electronics Specialists Conference, 2008. PESC 2008. IEEE* , pp. 269-272, 15-19 June 2008.

[2] J. Lu, F. P. Dawson and S. Yamada, "Application and Analysis of Adjustable Profile High Frequency Switch Mode Transformer Having a U-Shaped Winding Structure," *IEEE Trans. on Magnetics*, Vol. 34, No. 4, pp. 1345-1347, July. 1998.

[3] Z. Yanjun, X. Dehong, M. Kazuaki and S. Kiyoaki, "1MHz-1kW LLC Resonant Converter with Integrated Magnetics," *Applied Power Electronics Conference*, pp. 955-961, March 2007.

[4] C. Hangseok, "Analysis and Design of LLC Resonant Converter with Integrated Transformer," *Applied Power Electronics Conference*, vol., no., pp. 1630-1635, March 2007.

[5] B. Yang, R. Chen and F.C. Lee, "Integrated magnetic for LLC resonant converter," *Applied Power Electronics Conference and Exposition, 2002*, vol.1, pp. 346-351, 2002

[6] R. Chen, J. T. Stridom and J. D. van Wyk, "Design of planar integrated passive module for zero-voltage switched asymmetrical half bridge PWM converter," *Industry Applications Conference, 2001*, vol.4, pp. 2232-2237, Oct. 2001

[7] W. G. Hurley and D. J. Wilcox, "Calculation of Leakage Inductance in Transformer Windings", *IEEE Trans. on Power Electronics*, vol. 9, no. 1, pp. 121-126, Jan. 1994.

[8] N. Mohan, T. M. Undeland, and W. P. Robbins, Power Electronics: Converters, Applications, and Design, vol. 1, John Wiley & Sons, New York, NY, USA, 2003.

[9] S. R. Thondapu, M. B. Borage, Y. D. Wanmode and P. Shrivastava, "Improved Expression for Estimation of Leakage Inductance in E Core Transformer Using Energy Method", *Advances in Power Electronics*, vol. 2012, Article ID 635715, 2012.